

11A1-6

MZI-SOA based all-optical router implementation with OCDMA header recognition

P. Teixeira¹, L. Oliveira¹, T. Silveira^{1,2}, P. André¹, R. Nogueira¹, M. Lima¹, A. Teixeira¹

¹Instituto de Telecomunicações, Campus Universitário de Santiago 3810-193 Aveiro, Portugal

²Siemens Networks SA, Rua Irmãos Siemens 1, 2720-093 Amadora, Portugal

Phone: +351-234377900, Fax: +351-234377901, e-mail: pteixeira@av.it.pt, lmoliveira@av.it.pt, tiago.silveira@siemens.com, pandre@av.it.pt, mogueira@fis.ua.pt, mlima@det.ua.pt, teixeira@ua.pt.

Abstract — A router implementation based on OCDMA header recognition and MZI-SOA switching, allowing ps range packet switching capabilities is presented in this paper. Architecture and simulation results are presented.

I. INTRODUCTION

In this paper an all-optical router architecture is proposed, where the label detection is based on time domain Optical Code Division Multiple Access (OCDMA) header correlation. To perform routing, the data labels from different users/channels have to be detected and recognized in order to allow all-optical forwarding to the required port. An OCDMA packet header/trailer/label, unique for each route, is coded prior/following to each data packet. This label, by all-optical correlation identifies the port where to forward the packet, where a new or the same label can be added.

Fig. 1 illustrates the proposed router block diagram.

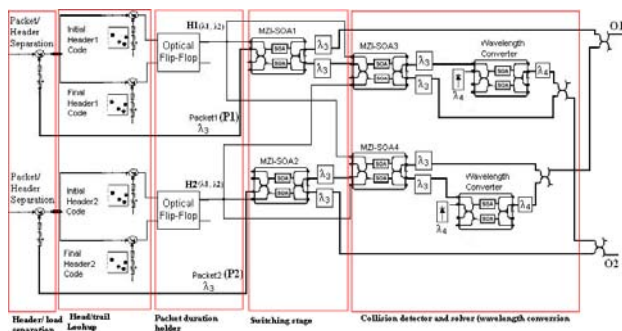


Fig. 1: All-optical router block diagram.

II. CODING SYSTEM

The encoders can be achieved by, eg., coding orthogonal sequences (eg. Kasami, Gold, Hadamard) with good auto- and cross-correlation properties in Super-Structured Fiber Bragg Gratings (SSBFG), while each decoder is achieved by writing the reversed code sequence of the matching encoder. This is a coherent bipolar system that uses the phase dimension to encode the header/trail [1]. The SSBFGs are divided into segments, one for each bit of the code sequence. Each different bit represents a different phase shift: 0 or π . Thus, between adjacent segments with different phase shifts, a phase discontinuity occurs on the grating periodic variation of the refractive-index modulation (Fig. 2).

Coding system performance can be evaluated by measuring the auto-correlation peak at the decoder output (Pa), the Pa to maximum wing level ratio (P/W) and the Pa to cross-correlation level (P/C). For low values of the grating refractive index, the relation between the grating spatial refractive index modulation profile and the impulse response shape is given by a Fourier-transform [2]. Thus, the refractive index must be kept low, which introduces a trade-off between high reflectivity (high Pa) and high P/W, P/C ratios. Though better correlation values can be obtained by using longer optical codes, the requirements of this system permit to partially disregard this constrain, maintaining system simplicity level. The simulations were run using two 16 chip Hadamard codes. Shorter chip length will achieve better pulse shape fidelity to the code, for the energy decaying effect along the grating [3], and thus higher P/W and P/C. Though, inter-symbolic interference effects due to dispersion are more important to shorter chip time. Hence, our choice is a chip length of 2.3mm which corresponds to a chip time of 22.2ps. Moreover, a minimum 125ps pulsewidth is required to trigger the flip-flops [5], so pulse broadening is needed in a following stage. A study of the coding system performance for different input pulsewidth values is presented in subsections a) and b). The study includes the effect of the apodization of the SSBFG.

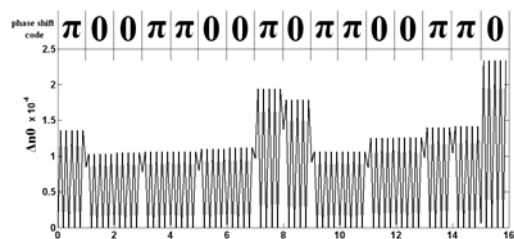


Fig. 2: Coder1 structure: refractive-index modulation apodized profile.

a) Apodization

The try-and-error method suggested in [1] was used to apodize the gratings. Here, the reflectivity of different chip along the grating is adjusted in order to maintain the pulse response peak variation within a small range. The apodization was designed for the maximum Pa, occurring at 16ps pulsewidth. The obtained apodization profile is shown in the grating structure depicted in Fig. 2.

In Fig. 3, Pa and P/W, P/C ratios are plotted versus the pulsewidth. Apodization performance is also shown. While the Pa maximum corresponds to 16ps, P/W and P/C present an overall tendency to decrease with pulsewidth as predicted in [4]. For 64ps, P/W shows an abnormal increase due to an observable code distortion by pulse overlapping within code, which introduces a higher

right-side wing whereas for all other pulsewidth, the higher wing is the one in the left.

The effect of apodization, also shown in Fig. 3, is to improve Pa and P/W, P/C ratios. For 16ps, the increase is about 5dB for Pa, 2dB for P/W and 1dB for P/C and the total power loss, measured as the ratio of auto-correlation peak to input pulse peak, is of 16.6dB for the apodized case and of 20.3dB for the non apodized.

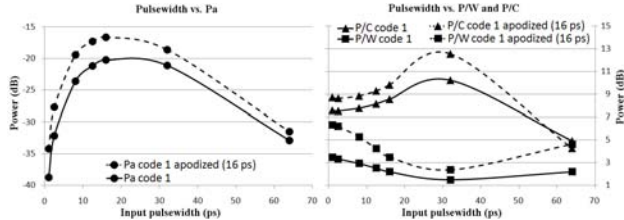


Fig. 3: OCDMA system: pulsewidth vs. performance.

b) Pulse expansion

Once the previous system cannot achieve 125ps wide pulses for flip-flop triggering, we use, after the decoder, a 60mm long apodized BFG acting as a pulse expander to convert the pulsewidth from 16ps to 130ps which introduces a power penalty of about 8dB.

II. THE SWITCH SUBSYSTEM

After correlation, the header becomes a pulse. Both initial and final header pulses are input into the RS flip-flop [5]. When correlated, the initial header sets on the flip-flop and the final header sets it off. During this time, the packet is all-optically switched in the switch subsystem.

The switch subsystem is divided in three MZI-SOA stages for each input. The first stage receives a packet and its respective header signal. This stage decides if the packet should be bar or cross ported, according to the existence or not of the header signal. In case of “not”, the packet will cross the switch by passing through a second MZI-SOA structure. The second stage receives the crossing packet and decides if the packet should be wavelength converted or not. The decision is based on the other packet header’s information. However this MZI-SOA does the XOR operation between the two header signals, since the XOR operation improves the packet pass-to-packet drop ratio (P1/P0) in about 10dB, according to the simulations. The third MZI-SOA stage is used to implement the wavelength converter.

One important aspect in the switch subsystem is the reminiscent power of the blocked packets. It can be an issue in the system performance. Since it is verified in every MZI-SOA stage, the effect can be cumulative and, consequently, increase the blocked packet power in the system output, making it comparable to the unblocked packet or increasing the crosstalk effect, degrading the unblocked packet.

Considering only output1, Fig.4 shows the variation of the P1/P0. The λ_0 (original wavelength) curve represents the variation of P1/P0 for both packets in the original wavelength. The λ_c (converted wavelength) curve

represents the same variation for packets that had to be wavelength converted. In (A), the difference, in the best case, between the original and converted wavelength are about 10dB. The crossing packet2 has to pass by the third MZI-SOA stage, decreasing the performance of the λ_c curve. Anyway, a P1/P0 of about 25dB is possible for the λ_0 curve, if the header powers are optimized. Even for the λ_c curve, P1/P0 of about 15dB is also a good result.

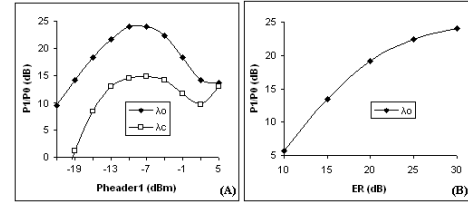


Fig. 4: Results for output1 (O1). (A) P1/P0 as a function of the header1 (H1) power when header2 (H2) power is fixed. (B) P1/P0 as a function of both headers Extinction Ratio (ER).

The results referred in Fig. 4 (A) considered the ER of both header signals as ideal. By varying the ER of both header signals, Fig. 4 (B) illustrates that, for output1, P1/P0 for the original wavelength packets decreases along with the ER of the header signals. The decreasing is mostly caused by the packets that are being bar ported, which are directly dependent of the corresponding header power. The packets that are crossing the switch, although in the same wavelength, pass through the XOR gate, which helps them to maintain the same amplitude.

III. CONCLUSION

A model to implement an all-optical router was demonstrated by means of simulation. It showed good performance in terms of Packet pass-to-Packet drop ratio. A study about the viability of using OCDMA encoding based on SSFBG to implement the headers correlators was made. It also showed promising results.

REFERENCES

- [1] X. Wang, A. Nishiki and K. Kitayama, “Improvement of the coding performance of SSFBG en/decoder by apodization technique”, *Microwave and Optical Techno. Lett.* 43, 247-250 (2004).
- [2] P. C. Teh, P. Petropoulos, M. Ibsen and D. J. Richardson, “A comparative study of the performance of seven and 63-chip optical code-division multiple-access encoders and decoders based on superstructured fiber Bragg gratings”, *J. Lightwave Technol.* 9,1352-1365 (2001).
- [3] X. Wang, K. Matsushima, A. Nishiki, N. Wada, and K. Kitayama, “High reflectivity superstructured FBG for coherent optical code generation and recognition”, *OSA Optics Express*, vol. 12, no. 12, pp. 5457-5468, November 2004.
- [4] K. Matsushima, X. Wang, S. Kutsuzawa, A. Nishiki, S. Oshiba, N. Wada and K. Kitayama, “Experimental demonstration of performance improvement of 127-Chip SSFBG en/decoder using apodization technique”, *IEEE Photonic Technol. Lett.* Vol. 16, No. 9, pp. 2192-2194, Sept. 2004.
- [5] R. McDougall, Y. Liu, G. Maxwell, M.T. Hill, R. Harmon, S. Zhang, L. Rivers, F.M. Huijskens, A. Poustie, H.J.S Dorren, “Hybrid Integrated, All-optical Flip-Flop Memory Element for Optical Packet Networks”, paper Th1.4.5, *ECOC2006*, Cannes, France, 2006.